Challenges and opportunities in constructing a near-field microwave microscope to image superconducting samples

Steven M. Anlage, Quantum Materials Center, Physics Department, University of Maryland

This document is intended solely for the use of students registered in Physics 798C, "Introduction to Superconductivity" at the University of Maryland during the Spring 2024 Semester

Statement of the Problem

What are the design challenges that must be addressed to build a near-field microwave microscope that will develop contrast in electrodynamic properties (e.g. surface resistance and surface reactance) from a superconducting sample? There are many considerations that come into play when designing a microwave microscope. We have to start with the sample and the type of contrast that we hope to develop from it, and then work backwards to see how a microscope can be designed to uncover this contrast. In this document we shall focus on <u>linear response</u> properties of the superconductors. As an alternative, one can design a microscope to measure local *nonlinear* properties of superconductors [see Ref. [1]], but this will not be discussed here.

Superconducting Electrodynamics

The samples of interest are superconducting. In general, these materials are inhomogeneous on several different length scales. These inhomogeneities are of interest to image and study. However, we will start with the assumption that the material is <u>uniform</u> and <u>homogeneous</u> and see what kind of response a microscope will develop in the presence of such a sample. It should be remembered that this is a kind of "worst case scenario," and that the real samples of interest probably will show more variable and interesting response. The electrodynamic properties of superconductors are described by their complex conductivity $\sigma = \sigma_1 - i\sigma_2$, where we adopt the $e^{+i\omega t}$ harmonic time convention. The complex conductivity can be calculated from Mattis-Bardeen theory,[2] or various generalizations that include the effects of quasiparticle lifetime,[3,4] proximity coupling, magnetic impurities, weak links, etc. We shall assume that the superconductor is local in the sense that the constitutive equation between electric field and current is simply $\vec{J} = \sigma\vec{E}$. Under these circumstances, one can relate the complex conductivity to the complex surface impedance as $Z_s = \sqrt{\frac{i\omega\mu_0}{\sigma}}$. The surface impedance is complex, $Z_s = R_s + iX_s$, where R_s is the surface resistance and X_s is the surface reactance. It represents the ratio of the tangential electric field to the tangential magnetic field at the surface of a flat and semi-infinite sample. Superconductors have a different electrodynamic response from normal metals, semiconductors and insulators due to the large value of $\sigma_2 \gg \sigma_1$, which results in $X_s \gg R_s$, usually (but not always!). The complex conductivity and surface impedance are generally strong functions of temperature, frequency, and sample geometry (i.e. constrictions in thickness and/or width). Note that the concept of surface impedance as a boundary condition on the electric and magnetic fields breaks down when the radius of curvature of the superconductor surface, or the current distribution in space, is less than or comparable to the penetration depth λ.[5] The complex conductivity σ is therefore a "more fundamental" property of superconductors than surface impedance.

Electric Tip Near-Field Microwave Microscope

We shall assume that an STM-tipped probe will be used to construct the microwave microscope. This immediately puts us in the class of "Electric Tip" probes by the classification scheme of Ref.[6] There is a characteristic length scale D associated with the tip. In the case of an STM tip we take D to be the diameter of an equivalent sphere that models the end of the tip and is the source of electric field lines that are concentrated on the sample surface immediately below the tip. There is a study of STM tips and their equivalent sphere size by Imtiaz and Anlage.[7]

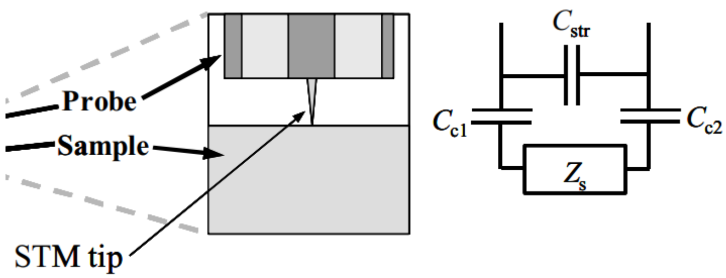

Figure 1. Figure 2 from Ref.[6] Close view of the coaxial probe, STM tip and sample, as well as a lumped element circuit model for the tip-sample interaction.

"In order to create a true near-zone or evanescent field in the sample, the tip characteristic size D must be small enough not only compared to the free-space wavelength λ_{EM}, but also to provide $|k_s|D \ll 1$, where $k_s = \omega\sqrt{\varepsilon_0\varepsilon_s\mu_0\mu_s}$ is the complex wave number for an electromagnetic wave in the material under test. In this case the tip-sample interaction can be viewed as a "cloud" of the probing electric or magnetic field penetrating the sample. The size of this cloud is on the order of the tip size D due to the static character of the near-field. Therefore the microscope spatial resolution—both lateral and in-depth—is mostly governed by the tip geometry rather than the electrodynamic properties of the sample."[6] The dielectric function of a superconductor is given by $\varepsilon_s = \varepsilon_{r,SC} - \frac{i\sigma}{\varepsilon_0\omega}$, where $\varepsilon_{r,SC}$ is the relative dielectric constant of the superconductor which gives rise to displacement currents. At microwave frequencies these currents are small compared to the physical currents, and so one typically neglects this term. We shall also assume that the superconductor is non-magnetic, hence $\mu_s = 1$. Exceptions to this include materials such as Gd-Ba-Cu-O, which have coexisting antiferromagnetism on the Gd sub-lattice and superconductivity in the Cu-O planes.[8,9] Writing out the complex conductivity, we have $\varepsilon_s = \frac{-1}{\varepsilon_0\mu_0\omega^2\lambda^2} - \frac{i\sigma_1}{\varepsilon_0\omega}$, where we have used the approximation that $\sigma_2 \approx \frac{1}{\mu_0\omega\lambda^2}$, and λ is the magnetic penetration depth. If we make the further assumption that $\sigma_2 \gg \sigma_1$, which is not always valid, we can write the approximate superconductor dielectric function as, $\varepsilon_s \approx \frac{-1}{\varepsilon_0 \mu_0 \omega^2 \lambda^2}$. Going back to the complex wavenumber calculation, we can now write $k_s \approx i/\lambda$, showing that the wave propagation inside the superconductor is evanescent, to good approximation, and the electromagnetic excitation in the superconductor decays on the scale of the penetration depth. Finally, to establish the condition $|k_s|D \ll 1$ requires that $D \ll \lambda$, which is a somewhat demanding requirement. In the case of a "typical" low carrier density superconductor we may have $\lambda = 200\, nm$. Hence the tip characteristic dimension D should be on the order of, say, $50\, nm$, or smaller. This would establish the conditions for "a true near-zone or evanescent field in the sample."[6]

Next is the question of the magnitude of the surface impedance of the superconductor. Here we take the approximation that the superconductor is in the local limit and that the surface impedance concept is still valid. In Ref.[6] it is shown that the bulk (i.e. a semi-infinite sample) impedance of the sample is given by the approximation $Z_{sb} \approx \frac{1}{i\omega\varepsilon_0\varepsilon_s D}$, "which is basically the impedance of a capacitor with a geometrical capacitance $\varepsilon_0 D$ filled up with material of complex relative permittivity ε_s."[6] If we again make the approximation that $\sigma_2 \gg \sigma_1$, which is not always valid, we can write the approximate superconductor dielectric function as, $\varepsilon_s \approx \frac{-1}{\varepsilon_0 \mu_0 \omega^2 \lambda^2}$. This leads to a surface impedance that is purely imaginary (i.e. inductive reactive), $Z_{sb} \approx i\mu_0\omega\frac{\lambda^2}{D}$, and is proportional to the tip-related effective penetration depth $\frac{\lambda^2}{D}$. Note that this differs from the usual expression for the effective penetration depth of a superconducting thin film of thickness t, $\lambda_{eff} = \frac{\lambda^2}{t}$, which is valid in the limit $t \ll \lambda$. In the near-field limit, the tip diameter partially sets the scale for penetration of electromagnetic fields into the superconductor, even in a bulk material.

It will turn out that increasing the magnitude of Z_{sb} will be desirable. To maximize the bulk superconducting impedance magnitude, one wants to maximize operating frequency ω, maximize the magnetic penetration depth λ (i.e. consider low carrier density materials and granular materials, or go to temperatures near T_c or frequencies near the gap frequency), and minimize the tip characteristic dimension D. Note that increasing the frequency comes at the price of increasing radiation loss from the electric-tip probe, and brings one closer to the spectroscopic energy gap of the superconductor, 2Δ.

Here we will estimate the magnitude of the surface impedance presented by various superconductors to the electric tip probe: $Z_{sb} \approx i\mu_0\omega\frac{\lambda^2}{D}$. First consider the case of a low-T_c bulk superconductor, such as Pb. Assume a frequency of 1 GHz, magnetic penetration depth of $\lambda = 52.5\, nm$,[10] and tip characteristic dimension of $D = 20\, nm$. One finds in this case that $Z_{sb} \approx i\ 1.1\, m\Omega$.

Next consider the case of a high-T_c bulk superconductor such as Bi2212. Assume a frequency of 1 GHz, an in-plane magnetic penetration depth of $\lambda = 200\, nm$ (this implicitly assumes that one is tunneling into the ab-planes from the c-direction), and tip characteristic dimension of $D = 20\, nm$. One finds in this case that $Z_{sb} \approx i\ 15.8\, m\Omega$. Tunneling into the side of a Bi2212 crystal from the a- or b-direction would involve the c-axis screening length, which is considerably larger than 200 nm, hence Z_{sb} would be larger, perhaps on the order of i 1 Ω.

Next consider the case of a granular superconductor such as granular Aluminum (GrAl). Assume a frequency of 1 GHz, magnetic penetration depth of $\lambda = 3.2\,\mu m$ (this is a film of thickness $t = 20\,nm$ with $L_{K/\square} = \mu_0 \frac{\lambda^2}{t} = 0.64\,nH/\square$ in Table I of Ref.[11]), and tip characteristic dimension of $D = 20\,nm$. One finds in this case that $Z_{sb} \approx i\,4.0\,\Omega$.

Model of Electric-Tip / Sample Interaction

Prior work with *transmission line resonator* microwave microscopes with an STM tip extension of the center conductor used a series lumped-element model of tip-sample interaction. It assumed that the tip-sample capacitance C_x is in series with the sample resistance R_x. It was found that the minimum Q of the resonator (a measure of good sensitivity to the sample properties) was at the point where $\omega R_x C_x = 1$.[12] This microscope design is not optimized for superconductor sample investigation, and the model is oversimplified, hence these results should be treated with caution. Nevertheless, it gives a general idea that there is a tradeoff between operating frequency, probe-sample capacitance, and the range of accessible sample loss values.

What are typical values of tip-sample capacitance C_x for STM tips over metallic samples? Imtiaz reports $C_x \approx 1 - 10\,fF$ for etched W tips at tunneling heights.[12] Tip-sample capacitance values on the order of $1\,fF$ were seen in another study.[13]

The lumped element model in Fig. 2 from Ref.[6] is shown above. The impedance Z_{tE} of the electric tip is given by $(Z_{tE})^{-1} = \left(\frac{1}{i\omega C_c} + Z_s\right)^{-1} + i\omega C_{str}$, where $1/C_c = 1/C_{c1} + 1/C_{c2}$ and Z_s is the sample impedance. "To obtain high enough sensitivity to the sample properties (i.e., to make $Z_{tE} \sim Z_s$), it is imperative to have both $1/\omega C_c Z_s$ and $\omega C_{str} Z_s$ much smaller than or at least on the order of unity." [6] The first condition depends on the tunneling height since in the case of an STM tip over a sample $C_c \approx C_x$. Since C_{str} (stray capacitance from the tip to ground) is generally "small", we expect the condition $\omega C_{str} Z_s \ll 1$ to be easily satisfied. For the first condition, take a frequency of 1 GHz, $C_x = 1 fF$, and $Z_s = 4.0\,\Omega$ (the case of GrAl). This yields $1/\omega C_c Z_s = 4 \times 10^4$, which does not satisfy the criterion that it be much less than unity. This means that the electric tip impedance is dominated by the tip-sample capacitance, rather than the sample impedance, even in the case of a granular superconductor. **This is the fundamental problem in probing low-impedance samples, such as superconductors, with an electric probe tip**. Such microscopes are basically scanning capacitance meters with virtually no sensitivity to superconducting microwave properties.

Possible approaches to mitigating this issue include increasing the tip-sample capacitance by going closer to the sample, increasing the operating frequency of the microscope, and increasing the sample impedance, perhaps by going to lower carrier density materials, and/or adding magnetic vortices. Note that making the tip characteristic dimension D smaller will serve to increase the sample impedance $Z_{sb} \approx i\mu_0\omega\frac{\lambda^2}{D}$, and decrease the tip-sample capacitance $C_x \propto \varepsilon_0 D$, hence it will probably not change the value of $1/\omega C_c Z_s$.

(Generally Unsuccessful) Approaches to Improving Electric-Tip Sensitivity to Superconductors

There are a number of methods that have been employed to improve the sensitivity of the microwave response signal to the tip-sample interactions. This includes the use of "impedance matching" techniques, and the idea of modulating the tip-sample distance periodically in time, and measuring the response at the modulation frequency to remove the effects of "stray capacitance".

Lumped LC circuit impedance matching

A number of groups have explored the idea of building an impedance matching circuit that serves to match the high impedance of the electric-tip probe to $50\,\Omega$. The radio-frequency scanning tunneling microscope uses a lumped LC-circuit to create a reflection zero in a "shunt-impedance" measurement configuration.[14] The main accomplishment of this paper is to utilize the STM tunnel barrier resistance R as a tunable parameter, combined with the fixed LC circuit elements, to create an LCR circuit that has a zero in S_{11} at a frequency in the 100 MHz range. It essentially maps the tip height z onto a strongly variable reflected voltage wave amplitude near the $S_{11} = 0$ condition. In some sense this is a step backwards because the DC tunnel current is more sensitive to z than the reflected RF signal, and this is evident in their topography images in Figs. 1(c) and (d). However, it enables the feedback loop to operate on an RF signal that has roughly 1-10 MHz of bandwidth, which is superior to the bandwidth of conventional DC tunnel current based feedback loops. However, they do not experimentally demonstrate any advantage to the higher bandwidth in the paper. They make no claims about sensitivity to sample properties, other than topography of Au surfaces.

As an aside, the RF-STM approach brings up the question of how to model the tip-to-sample impedance. In STM, one thinks of the vacuum barrier as providing a resistance R that depends on the probe-sample separation z. At microwave frequencies we look at the same situation and see a probe-sample capacitance, and see a displacement current across that gap. In fact, at finite frequency both channels act in parallel, creating $Z_{Tunnel\ Barrier} \approx \left(\frac{1}{R} + i\omega C_x\right)^{-1}$. At low frequencies where STM is done, the resistance carries the current, while at high frequencies the current will flow mainly through the capacitor.

The PrimeNano approach to impedance matching utilizes a 1/4-wave stub tuner.[15] The impedance matching circuit creates a strong response from the probe/sample combination at one frequency, but does not change the physics of the probe-sample interaction discussed above. The use of a cancellation signal to null the background signal is also a good idea,[15] but it does not alter the physics of the probe/sample interaction. Note that in Ref.[15] they acknowledge this basic fact: "Similar to other microwave microscopes, no contrast will show up in the resistive channel if the sample is insulating or a perfect metal,[21]" where Ref. 21 are two papers by Atif Imtiaz.[7,12] Figure 2 of this paper[16] has a nice summary of MIM images for very low and very high sheet resistance samples. In the low sheet resistance sample the capacitance image is very clear while the resistive image has very little contrast.

The bottom line is that I do not see how an impedance matching circuit can overcome the issue of tip-sample capacitance dominating the response of the microscope tip.

Oscillating the tip-sample separation

An alternative method to gather information from the tip-sample interaction is achieved by means of modulating the tip-sample distance in time.[17,18,19,20] One then recovers a signal at the tip modulation frequency in order to eliminate background scattering from the tip, sample, stray capacitance, etc. The signals are taken from a lock-in at the modulation frequency, and represent the z-derivatives of transmission magnitude and phase, in the case of Keilmann.[18] The resulting signal arises from the near-tip and sample interaction, and this serves to improve the spatial resolution of the images. However, if the impedance of the C_x capacitor dominates Z_{tE}, then the modulated signal only seems to reflect the time-dependence of C_x. This modulation will not change the balance between the tip-sample capacitance and the sample impedance. For more detail, look at the work of Fritz Keilmann, and other papers by the early STM microwave microscopy folks.

Other ways to enhance superconductor loss to create contrast in an electric-tip near-field microwave microscope

In all of the above discussion we have ignored the contribution of σ_1 to the dielectric function and surface impedance. The question arises: how can we make the magnitude of σ_1 large in the superconducting state? In fully-gapped superconductors $\sigma_1 \to 0$ in the limit of zero temperature. In reality, all superconductors have sources of residual loss that prevent the real part of the conductivity from reaching zero. This intrinsic loss can become large (on the order of the normal state conductivity σ_n) in gapless superconductors, created (for example) by magnetic impurities in s-wave superconductors. In nodal superconductors one might expect an intrinsic non-zero residual value of σ_1 due to the nodes, in the limit of zero temperature. In line-nodal superconductors (such as the cuprates) one has a universal residual σ_1 given by $\sigma_{00} = \frac{ne^2\hbar}{m\Delta_d}$, as derived by Hirschfeld.[21] In point-nodal superconductors there is also a finite residual σ_1, but it does not have a universal value, according to Hirschfeld (private discussion). Note that losses are also enhanced when strong currents flow in the superconductor, and this can be brought about by geometrically constraining the current flow in the superconductor by decreasing D, film thickness, or patterned film width.

We can calculate the bulk impedance of the superconductor keeping the real part of the conductivity in the dielectric function expression. The result is given by $Z_{sb} \approx i\mu_0\omega\frac{\lambda^2}{D}\left[1 - i\frac{\sigma_1}{\sigma_2}\right]$, where it is assumed that $\sigma_2 = \frac{1}{\mu_0\omega\lambda^2} \gg \sigma_1$. Hence, we can write $Z_{sb} = R_{sb} + iX_{sb}$, with $R_{sb} = \frac{\sigma_1}{D}(\mu_0\omega\lambda^2)^2$ and $X_{sb} = \mu_0\omega\frac{\lambda^2}{D}$. Going back to the electric-tip impedance $Z_{tE} \approx \frac{1}{i\omega C_c} + Z_{sb}$, and assuming that $X_{sb} \ll \frac{1}{\omega C_c}$, we have $Z_{tE} \approx \frac{1}{i\omega C_c} + R_{sb} = \frac{1}{i\omega C_c} + \frac{\sigma_1}{D}(\mu_0\omega\lambda^2)^2 = R_{tE} + iX_{tE}$. We can now go back to Ref.[6] and calculate the Q of a transmission line resonator terminated with an electric tip, Eq. (17). We make the approximation that $X_{tE} \gg R_{tE}$, and the Q expression simplifies to $Q \approx \frac{\pi n + Z_0/X_{tE}}{2\, h'' L + 2 Z_0 R_{tE}/X_{tE}^2}$, where n is a positive integer (mode number of the transmission line resonator), Z_0 is the characteristic impedance of the transmission line, and h'' is the imaginary part of the propagation constant of the transmission line of length L. This argues for making $Z_0/X_{tE} \gg 1$ to maximize the Q and to help make the $2Z_0 R_{tE}/X_{tE}^2$ term dominate over the $2\, h'' L$ term in the denominator. Further, one would have to use a short superconducting transmission line resonator with vacuum, or other low-loss, dielectric to minimize the $2\, h'' L$ term. Under these circumstances one would develop contrast in the Q of the microwave microscope associated with variations in σ_1 of the sample. Variations in the reactance X_{sb} may show up as changes in the resonant frequency.

Another source of contrast in superconducting samples will come from magnetic vortices in the material. A microwave microscope has measured the nonlinear response associated with Josephson vortices in a cuprate thin film grain boundary.[22,23] A single magnetic vortex will introduce both resistive and reactive contributions to the surface impedance presented by the superconductor to the electric tip microscope. The traditional approach to calculating the impedance of a large collection of magnetic vortices is the work of Gittleman and Rosenblum,[24] later updated by Coffey and Clem.[25] These approaches do not address the loss and reactance of individual vortices.[26] However, the core of the vortex is essentially normal conducting, at least in classical low-T_c superconductors. Hence it should present $\sigma_1 \sim \sigma_n$ to the microscope when positioned over the vortex core. Imaging vortices by means of their enhanced microwave losses and reactance is an interesting opportunity, and we are not aware of any work in this area.

Question the Assumptions!

The above estimates are made under a number of approximations which are not always valid, or may be circumvented in some situations. The main assumption is that we are using an "electric tip" probe, and that the near-field quasi-static electrodynamic fields are achieved in the sample. Another assumption is that the surface impedance boundary condition concept is valid. We have also assumed that the superconductor is in the bulk limit and does not have any geometrical constraints (such as thickness and width) that can enhance the microwave current values and increase the magnitude of the effective impedance.

Acknowledgement: I have benefitted greatly from discussions with Dr. Vladimir Talanov.

References:

1 Bakhrom Oripov, Thomas Bieler, Gianluigi Ciovati, Sergio Calatroni, Pashupati Dhakal, Tobias Junginger, Oleg B. Malyshev, Giovanni Terenziani, Anne-Marie Valente-Feliciano, Reza Valizadeh, Stuart Wilde, and Steven M. Anlage, "High-Frequency Nonlinear Response of Superconducting Cavity-Grade Nb Surfaces," Physical Review Applied **11** (6), 064030 (2019).

2 D. C. Mattis and J. Bardeen, "Theory of the Anomalous Skin Effect in Normal and Superconducting Metals," Phys Rev **111** (2), 412-417 (1958).

3 W. Zimmermann, E. H. Brandt, M. Bauer, E. Seider, and L. Genzel, "Optical conductivity of BCS superconductors with arbitrary purity," Physica C: Superconductivity **183** (1), 99-104 (1991).
4 Takayuki Kubo, "Effects of Nonmagnetic Impurities and Subgap States on the Kinetic Inductance, Complex Conductivity, Quality Factor, and Depairing Current Density," Physical Review Applied **17** (1), 014018 (2022).
5 Cougar AT Garcia, Nancyjane Bailey, Chris Kirby, Joshua A Strong, Anna Yu Herr, Steven M Anlage, and Vladimir V Talanov, "Disentangling superconductor and dielectric microwave losses in sub-micron $\rm Nb $/$\rm TEOS-SiO_2 $ interconnects using a multi-mode microstrip resonator," arXiv preprint arXiv:2303.10685 (2023).
6 Steven M. Anlage, Vladimir V. Talanov, and Andrew R. Schwartz, "Principles of Near-Field Microwave Microscopy", in *Scanning Probe Microscopy: Electrical and Electromechanical Phenomena at the Nanoscale*, edited by S. V. Kalinin and A. Gruverman (Springer-Verlag, New York, 2006), Vol. Vol. 1, pp. 207-245.
7 A. Imtiaz and S. M. Anlage, "Effect of tip geometry on contrast and spatial resolution of the near-field microwave microscope," J Appl Phys **100** (4), 044304 (2006).
8 L. V. Mercaldo, V. V. Talanov, and S. M. Anlage, "Microwave electrodynamics of the antiferromagnetic superconductor GdBa2Cu3O7-delta.," Physica C **341**, 1675-1676 (2000).
9 R. J. Ormeno, C. E. Gough, and Guang Yang, "Antiferromagnetic alignment and relaxation rate of Gd spins in the high temperature superconductor ${\mathrm{GdBa}}_{2}{\mathrm{Cu}}_{3}{\mathrm{O}}_{7\ensuremath{-}\ensuremath{\delta}}$," Phys Rev B **63** (10), 104517 (2001).
10 C. Egloff, A. K. Raychaudhuri, and L. Rinderer, "Penetration of a magnetic field into superconducting lead and lead-indium alloys," J Low Temp Phys **52** (1), 163-185 (1983).
11 Aviv Glezer Moshe, Eli Farber, and Guy Deutscher, "Granular superconductors for high kinetic inductance and low loss quantum devices," Appl Phys Lett **117** (6), 062601 (2020).
12 A. Imtiaz and S. M. Anlage, "A novel STM-assisted microwave microscope with capacitance and loss imaging capability," Ultramicroscopy **94** (3-4), 209-216 (2003).
13 Shu Kurokawa and Akira Sakai, "Gap dependence of the tip-sample capacitance," J Appl Phys **83** (12), 7416-7423 (1998).
14 U. Kemiktarak, T. Ndukum, K. C. Schwab, and K. L. Ekinci, "Radio-frequency scanning tunnelling microscopy," Nature **450** (7166), 85-88 (2007).
15 K. Lai, W. Kundhikanjana, M. Kelly, and Z. X. Shen, "Modeling and characterization of a cantilever-based near-field scanning microwave impedance microscope," Rev Sci Instrum **79** (6), 063703 (2008).
16 W. Kundhikanjana, K. J. Lai, H. L. Wang, H. J. Dai, M. A. Kelly, and Z. X. Shen, "Hierarchy of Electronic Properties of Chemically Derived and Pristine Graphene Probed by Microwave Imaging," Nano Lett **9** (11), 3762-3765 (2009).
17 A. Kramer, F. Keilmann, B. Knoll, and R. Guckenberger, "The coaxial tip as a nano-antenna for scanning near-field microwave transmission microscopy," Micron **27** (6), 413-417 (1996).
18 B. Knoll, F. Keilmann, A. Kramer, and R. Guckenberger, "Contrast of microwave near-field microscopy," Appl Phys Lett **70** (20), 2667-2669 (1997).

19 A. Tselev, S. M. Anlage, H. M. Christen, R. L. Moreland, V. V. Talanov, and A. R. Schwartz, "Near-field microwave microscope with improved sensitivity and spatial resolution," Rev Sci Instrum **74** (6), 3167-3170 (2003).
20 K. Lai, W. Kundhikanjana, H. Peng, Y. Cui, M. A. Kelly, and Z. X. Shen, "Tapping mode microwave impedance microscopy," Rev Sci Instrum **80** (4), 043707-043703 (2009).
21 P. J. Hirschfeld, W. O. Putikka, and D. J. Scalapino, "Microwave conductivity of d-wave superconductors," Phys Rev Lett **71** (22), 3705-3708 (1993).
22 Sheng-Chiang Lee and Steven M. Anlage, "Spatially-resolved nonlinearity measurements of YBa[sub 2]Cu[sub 3]O[sub 7-δ] bicrystal grain boundaries," Appl Phys Lett **82** (12), 1893-1895 (2003).
23 S. C. Lee, S. Y. Lee, and S. M. Anlage, "Microwave nonlinearities of an isolated long YBa2Cu3O7-delta bicrystal grain boundary," Phys Rev B **72** (2), 024527 (2005).
24 Jonathan I. Gittleman and Bruce Rosenblum, "Radio-Frequency Resistance in the Mixed State for Subcritical Currents," Phys Rev Lett **16** (17), 734-736 (1966).
25 J. R. Clem and M. W. Coffey, "Viscous Flux Motion in a Josephson-Coupled Layer Model of High-Tc Superconductors," Phys Rev B **42** (10), 6209-6216 (1990).
26 M. Checchin, M. Martinello, A. Grassellino, A. Romanenko, and J. F. Zasadzinski, "Electron mean free path dependence of the vortex surface impedance," Superconductor Science and Technology **30** (3), 034003 (2017).